

01 Jan 2004

## Highest-Quality Modes in Disordered Photonic Crystals

Alexey Yamilov

Missouri University of Science and Technology, yamilov@mst.edu

Hui Cao

Follow this and additional works at: [https://scholarsmine.mst.edu/phys\\_facwork](https://scholarsmine.mst.edu/phys_facwork)

 Part of the [Physics Commons](#)

---

### Recommended Citation

A. Yamilov and H. Cao, "Highest-Quality Modes in Disordered Photonic Crystals," *Physical Review A*, American Physical Society (APS), Jan 2004.

The definitive version is available at <https://doi.org/10.1103/PhysRevA.69.031803>

This Article - Journal is brought to you for free and open access by Scholars' Mine. It has been accepted for inclusion in Physics Faculty Research & Creative Works by an authorized administrator of Scholars' Mine. This work is protected by U. S. Copyright Law. Unauthorized use including reproduction for redistribution requires the permission of the copyright holder. For more information, please contact [scholarsmine@mst.edu](mailto:scholarsmine@mst.edu).

## Highest-quality modes in disordered photonic crystals

Alexey Yamilov\* and Hui Cao

Department of Physics and Astronomy, Northwestern University, Evanston, Illinois 60208, USA

(Received 25 July 2002; published 16 March 2004)

We studied the modes of the highest-quality factor  $Q_m$  in disordered photonic crystals. By varying the strength of disorder, we identified five different scaling regimes of the ensemble averaged  $\langle Q_m \rangle$  with the system size. For sufficiently large systems,  $\langle Q_m \rangle$  reaches the maximum at some finite degree of disorder, where its value is comparable to the quality factor of an intentionally introduced single defect at the center of a photonic band gap. Near this optimal degree of disorder, we predict a superexponential increase of  $\langle Q_m \rangle$  with the system size, due to migration of the frequencies of the highest-quality modes toward the photonic band-gap center. Our result may lead to the design and fabrication of ultralow-threshold random laser.

DOI: 10.1103/PhysRevA.69.031803

PACS number(s): 42.55.Ah, 42.25.Dd, 42.70.Qs

In a random laser, the feedback is provided by scattering instead of reflection [1–3]. The unconventional feedback mechanism of a random laser leads to properties interesting from both fundamental and practical points of view [1–12]. However the current threshold of random laser is still too high for many practical applications. In this paper we will show that the random laser threshold can be significantly reduced by incorporating some degree of order into an active random medium. We demonstrate that there exists an optimal degree of order/disorder where the random laser threshold is comparable to that of single-defect photonic band-gap laser [13]. This finding may lead to the design and fabrication of ultralow-threshold random lasers.

A finite open system of scattering particles can be characterized by a set of quasistationary (leaky) optical modes. When optical gain is introduced to such a system and is sufficient to compensate the leakage in at least one mode, lasing occurs. Thus the mode with the smallest leakage or highest quality tend to lase first, and its quality factor  $Q_m$  would determine the lasing threshold. However, the random lasing threshold also depends on many other factors. A realistic estimate should involve the detailed account of the gain material properties and its spatial distribution, the variation of the local density of states in the system and its effect on light-matter interaction, the pumping scheme, the reabsorption of laser light, etc. Therefore finding the threshold of random laser theoretically is a complicated problem. Nevertheless, in the case of a uniform gain distribution  $Q_m$  is the determining factor [8,9]. In this paper, we calculated the ensemble averaged  $\langle Q_m \rangle$  in two-dimensional (2D) open systems of square geometry, and studied its dependence on the degree of ordering and the system size  $L$ . With increasing strength of disorder, we gradually changed the systems from perfectly ordered photonic crystals to completely random media. During this transition, we identified five scaling regimes of  $\langle Q_m \rangle$  versus  $L$ : (a) photonic band edge,  $L^3$ , (b) transitional superexponential, (c) band-gap-related exponential, (d) diffusive,  $L^2$ , and (e) disorder-induced exponential, due to Anderson localization, regimes.

In disordered photonic crystals one cannot take simplify-

ing assumptions such as independent scattering approximation (low-density limit), or neglect the finite size of the scatterers. Moreover, the highest-quality modes weakly contribute to the transport properties of the system. Among other methods [14,15], finite difference time domain (FDTD) method has been shown to be a convenient tool in studying random laser modes in 1D [8] and 2D [9]. In this work, we used the FDTD method to find the highest-quality modes in open passive 2D random systems with various degrees of ordering. Our main results can be summarized as follows: (i) for sufficiently wide band gaps,  $\langle Q_m \rangle$  reaches a maximum at some finite strength of disorder; (ii) at this “optimal” degree of disorder,  $\langle Q_m \rangle$  is determined by the localization length similar to that of single defect in the ordered structure, leading to a similar quality factor; (iii) with an increase of the system size the optimal disorder strength decreases; (iv) near this optimal disorderness,  $\langle Q_m \rangle$  should scale superexponentially with the sample size, owing to the frequency migration of the highest-quality modes toward the band-gap center and the decrease of their localization lengths.

We consider a 2D  $L \times L$  (up to  $9\lambda \times 9\lambda$ ) photonic crystal made of  $N(\propto L^2)$  cylinders with diameter  $d=98$  nm and refractive index  $n_0=2.2$ . The cylinders were arranged into hexagonal lattice with nearest-neighbor distance  $a=140$  nm. In the absence of disorder, the infinite system with these parameters has full band gap in [361 nm, 426 nm] range for TM modes (electric field along the cylinder axis). The disorder in the system was introduced in two ways: by uniformly randomizing the refractive index  $n$  of different cylinders in the range  $[n_0 - w_n(n_0 - 1), n_0 + w_n(n_0 - 1)]$  and diameter  $[d(1 - w_d), d(1 + w_d)]$ . Care was taken to avoid the uncontrollable disorder due to discretization of the grid. Disorder in the system was characterized with parameter  $\delta\varepsilon = \langle \int [\varepsilon(\mathbf{r}) - \varepsilon_0(\mathbf{r})]^2 d\mathbf{r} \rangle^{1/2} / (\int \varepsilon_0^2(\mathbf{r}) d\mathbf{r})^{1/2}$ , where  $\varepsilon_0(\mathbf{r})$  and  $\varepsilon(\mathbf{r})$  are the dielectric constant distributions in ordered and disordered samples respectively.  $\langle \dots \rangle$  stands for the average over different disorder configurations. In the present work we studied the systems with 11 different disorder strengths: 1–10 had  $w_n$  from 0.1 to 1.0 with the increment 0.1 and  $w_d=0$ , the 11th had  $w_n=1.0$  and  $w_d=0.43$ . This led to variations of dielectric constant from weak  $\delta\varepsilon=0.08$  to strong  $\delta\varepsilon=0.95$  disorder. Later we will discuss the effect of this particular choice of the types of disorder. To mimic an open system, a buffer

\*Electronic address: a-yamilov@northwestern.edu

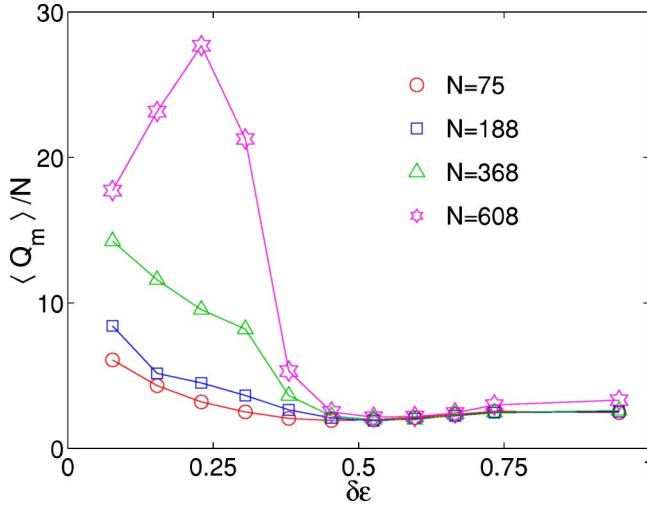


FIG. 1.  $\langle Q_m \rangle$  normalized by total number of scatterers  $N(\propto L^2)$  as a function of disorderness  $\delta\epsilon$ .

layer of air (150 nm thick) was kept around the sample, followed by uniaxial perfectly matched absorbing layers [16]. To excite the system we initially launched a short  $\sim 10$  fs pulse at every grid point. The frequency  $\omega_e$  of the pulse was at the center of the band gap (391 nm) of the ordered structure. In the frequency domain the full width at half maximum of the excitation pulse was of the order of the band-gap width. Thus the pulse excited all the modes within the stop band and near the band edges.

Right after the initial pulse, the competition between the modes [7,17] with different lifetimes led to the complicated evolution of total electric energy  $\mathcal{E}(t) = \frac{1}{2} \int \varepsilon(\mathbf{r}) \mathbf{E}^2(\mathbf{r}) d\mathbf{r}$ . However, after a sufficient time only the mode with the longest lifetime (highest-quality factor) survived.  $\mathcal{E}(t)$  followed a monoexponential decay  $\text{Re}[\exp 2i\omega_m(1+i/2Q_m)t]$ , from which we extracted the frequency  $\omega_m$  and quality factor  $Q_m$  of the longest-lived mode in this particular realization of disorder. At the same time the spatial pattern,  $\mathbf{E}(\mathbf{r})$ , was stabilized and the mode profile could be seen. Generally, the time needed to reach the monoexponential decay regime varied from about 0.5 ps for the smallest system to 10 ps for the largest. Finally,  $Q_m$  was averaged over 1000 ( $N=75$ ), or 100 ( $N=137, 188, 261, 368, 449, 608$ ) disorder realizations.

Figure 1 shows the dependence of  $\langle Q_m \rangle$  normalized by  $N$  as a function of the disorderness  $\delta\epsilon$ , different curves correspond to different system sizes. This particular normalization makes it easy to see the deviation from diffusion predicted [1] dependence  $\langle Q_m \rangle \propto L^2 \propto N$ . One can see that significantly different scalings at different  $\delta\epsilon$  lead to a maximum of  $\langle Q_m \rangle$  at the finite disorder strength. Figure 2 plots the size dependence of  $\langle Q_m \rangle$  for the fixed disorder strengths.

The understanding of this behavior comes from observing the frequencies  $\omega_m$  of the highest-quality modes in Fig. 3. For small  $\delta\epsilon$  the frequencies are concentrated at lower (long-wavelength) band edge, and they (as well as  $Q_m$ ) are independent of the frequency  $\omega_e$  of the excitation pulse. The reason for that is the way the disorder was introduced into the system. The long-wavelength modes are mostly concentrated in the dielectric cylinders, which are disordered by the

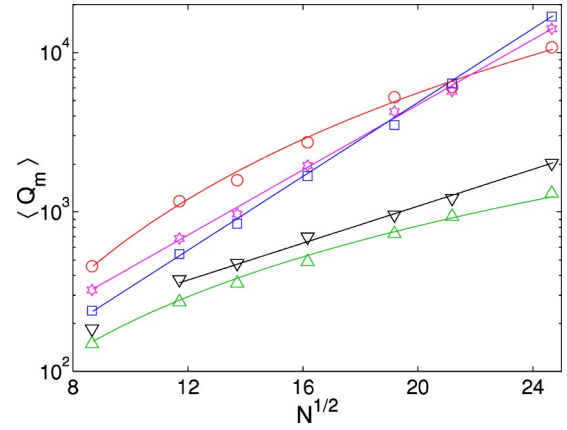


FIG. 2. Scaling of  $\langle Q_m \rangle$  with the lateral size of 2D system  $L \propto N^{1/2}$  in five regimes: band-edge  $L^3$  (circles); transitional superexponential (stars); band-gap exponential (squares); diffusion  $L^2$  (triangles); and disorder exponential (inverted triangles). The data points correspond to  $w_n=0.1$  ( $\delta\epsilon \approx 0.08$ ),  $w_n=0.2$  ( $\delta\epsilon \approx 0.15$ ),  $w_n=0.3$  ( $\delta\epsilon \approx 0.23$ ),  $w_n=0.7$  ( $\delta\epsilon \approx 0.53$ ), and  $w_n=1.0$  and  $w_d=0.43$  ( $\delta\epsilon \approx 0.95$ ) values of disorder parameter.

refractive index fluctuations. At  $w_n=0.1$ ,  $\omega_m$  fell in the immediate vicinity of the band edge [Fig. 3(a)]. Lasing from the band-edge modes was well studied in the case of ordered structures [12,18–22], with  $Q_m \propto L^3$  [12]. The latter indeed gives a good fit of our results.

At the increased disorder (Fig. 2),  $w_n=0.2-0.3$ , the dependence of  $\langle Q_m \rangle$  on the system size  $L$  became exponential, as expected for localized modes [10]. In the unit of wavelength the localization length  $\xi$ , obtained by fitting, decreased from  $1.44\lambda$  to  $1.27\lambda$  as  $w_n$  increased from 0.2 to 0.3. Figure 3(b) provides an insight into the physics behind the varying  $\xi$ . The quality factor can be estimated as  $\langle Q_m \rangle \propto \exp[L/2\xi(\omega_m)]$ , where  $\xi(\omega_m)$  is the “typical” value of the localization length at the frequency  $\omega_m$ . From Fig. 3(b) one can see that even for the same disorder strength, the increase in system size leads to the advance of  $\omega_m$  toward the band-gap center, where  $\xi$  is the smallest. This peculiar behavior should lead to superexponential dependence of  $\langle Q_m \rangle$  on  $L$  even for fixed disorder strength. The frequency migration with the increase of the system size can be explained by the fact that in the small system it is unlikely to find the modes deep into the band gap due to low density of states there. The Urbach-like behavior can be expected [14,23]. This is also qualitatively supported by Fig. 3(b) where the exponential dependence is apparent. Assuming Urbach-like dependence of the density of states, the advancement of  $\omega_m$  can be estimated from the condition that total number of defect states (proportional to the number of cylinders  $N$ ) times the probability of having a state located  $\Delta\omega(N)$  away from the band edge,  $\exp[-\alpha(\delta\epsilon)\Delta\omega(N)]$ , is equal to one. Here,  $\alpha(\delta\epsilon)$  is the exponential slope of the density of states, which should decrease with the increase of the disorder  $\delta\epsilon$ . For small disorder  $\alpha^{-1}(\delta\epsilon) \ll \Delta E_{PBG}$ , where  $\Delta E_{PBG}$  is the width of the photonic band gap. Therefore, for weak disorder (or small system size) the band-edge-type modes have the highest  $Q$ . The crossover to the superexponential dependence of  $\langle Q_m \rangle$  occurs when the  $Q$  of the localized states with the

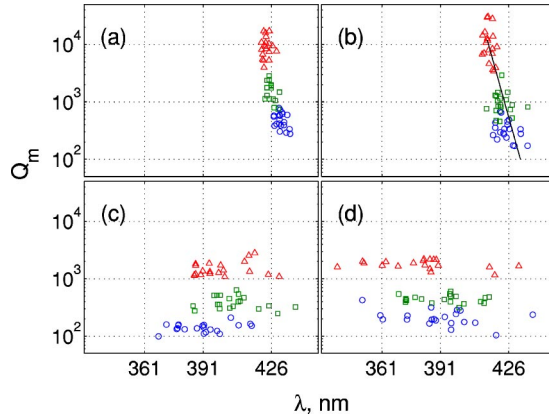


FIG. 3.  $Q_m$  vs cavity mode frequency for 20 realizations of disorder. Circles, squares, and triangles correspond to  $N$  equal to 75, 188, and 608, respectively. Four graphs correspond to different disorder parameters: (a)  $w_n=0.1$  ( $\delta\varepsilon \approx 0.08$ ), (b)  $w_n=0.2$  ( $\delta\varepsilon \approx 0.15$ ), (c)  $w_n=0.6$  ( $\delta\varepsilon \approx 0.45$ ), (d)  $w_n=1.0$  and  $w_d=0.43$  ( $\delta\varepsilon \approx 0.95$ ).

shortest localization length  $\xi[\Delta\omega(N)]$  available for this size  $N$  exceeds that of the band-edge-type mode:  $\exp[N^{1/2}a/2\xi[\Delta\omega(N)]] \sim N^{3/2}$ . Stronger size dependence in the superexponential regime means that the  $N^{3/2}$  band-edge-type dependence observed at smaller disorder would eventually switch to the superexponential dependence as  $N$  increases. However, the latter can be expected to saturate at larger size or disorder when  $\omega_m$  reaches the band-gap center:  $N[\exp[-\alpha(\delta\varepsilon)\Delta E_{PBG}/2]] \sim 1$ , where the localization length is the smallest. Therefore, we expect the limiting scaling of  $\langle Q_m \rangle$  to be exponential:  $\langle Q_m \rangle \propto \exp[N^{1/2}a/2\xi(\Delta E_{PBG}/2)]$ . Three important conclusions (i)–(iii) listed in the introduction immediately follow. (iii) is justified because  $\xi(\Delta E_{PBG}/2)$  is the smallest in the ordered structure. The saturated exponential dependence can be seen in our example for  $w_n=0.3$  (the squares in Fig. 2).

In our system the sharp drop in  $\langle Q_m \rangle$  at  $\delta\varepsilon \approx 0.4$  in Fig. 1 is attributed to the removal of the band gap. This could be seen from the loss of the hexagonal symmetry of the observed mode profiles as well as the sensitivity of the modes to the excitation pulse position  $\omega_e$ . In this regime,  $\omega_m$  is not associated with the photonic band gap, which does not exist anymore. However, in order to make a direct comparison with the ordered case, we kept the excitation pulse the same as before. The exact cause of the disappearance of the band gap is being debated in the literature [14,23,24], and is not the subject of this study. In our particular case we found a simple explanation for the behavior of  $\langle Q_m \rangle$  in the way the disorder was introduced. Indeed, the fluctuating index of refraction leads to the fluctuation of the frequency of the Mie resonances of the particles. For box distribution of  $n$ , there exists a value of  $w_n=0.6$  when the Mie resonance of some defect cylinders falls into the gap (Fig. 4). This value matches the value of disorder parameter  $\delta\varepsilon$ , where the sharp decrease of  $\langle Q_m \rangle$  is observed in Fig. 1. Moreover, Fig. 3(c) shows that at this crossover disorder, the modes avoid the region of strong single-particle scattering. This is the consequence of the sharp boundary in the distribution of  $n$ . It also indicates the presence of the residual band gap, where  $\omega_m$  are concentrated.

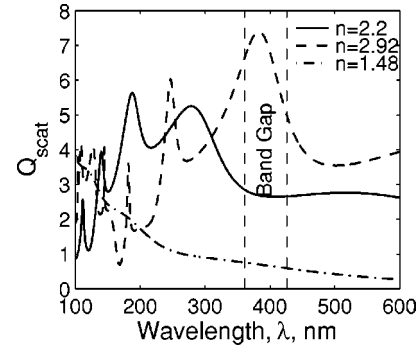


FIG. 4. Mie scattering efficiency vs wavelength for cylinders of diameter 98 nm. Refractive index  $n=2.2$  (solid line). For  $w_n=0.6$  ( $\delta\varepsilon \approx 0.45$ ), the refractive index fluctuates from  $n=1.48$  (dash-dotted line) to  $n=2.92$  (dashed line).

At  $w_n \geq 0.7$  the photonic band gap ceased to exist. Triangles in Fig. 2 correspond to  $w_n=0.7$ , and were successfully fitted with diffusion [1,4,5,12,25,26] scaling dependence:  $\langle Q_m \rangle \propto L^2 \propto N$ . Deviations from this dependence can be seen in Figs. 1 and 2 at the largest sizes studied, where  $L > \xi_{Anderson} = 2.54 \lambda$  and the states become localized again due to Anderson localization [10,12]. The exponential dependence of  $\langle Q_m \rangle$  on  $L$  becomes especially pronounced at the largest disorder studied (see inverted triangles in Fig. 2), where the transition from  $L^2$  to exponential dependence comes at small system sizes. We want to point out that even at such strong disorder, the obtained modes had a collective nature, rather than the single particle's high-order resonances, which were concentrated at higher frequencies. Comparing the localization length of these states to that of band-gap nature we see a factor of 2 difference, which makes the latter preferable (Fig. 1).

In conclusion, we studied the modes of the highest quality factor  $Q_m$  in disordered photonic crystals. By varying the disorder strength, we identified five scaling regimes for the ensemble averaged  $\langle Q_m \rangle$  versus the system size  $L$ . Difference in scaling results in a maximum of  $\langle Q_m \rangle$  at “optimal” disorder. Migration of the frequencies of highest-quality modes towards the center of the residual band gap could lead to superexponential scaling. We also predicted the “optimal” disorderness would decrease with increase of the system size. These results can be applied to 2D photonic crystals and film-based random lasers. Note that we only calculated the average values of the highest-quality factors  $Q_m$ . Since  $Q_m$  is a fluctuating quantity, a better description of it requires the calculation of its distribution and variance, which will be done in the future. Nevertheless,  $\langle Q_m \rangle$  is an important physical parameter. In fact our study provides a physical insight into recent experimental results of Shkunov *et al.*, Ref. [27]. The authors observed much lower threshold of lasing in defect modes associated with photonic band gap in disordered opals.

A. L. Burin is acknowledged for fruitful discussions. This work is supported by the National Science Foundation under Grant No. DMR-0093949. H.C. acknowledges the support from the David and Lucile Packard Foundation.

- [1] V. S. Letokhov, Zh. Eksp. Teor. Fiz. **53**, 1442 (1967) [Sov. Phys. JETP **26**, 835 (1968)].
- [2] V. M. Markushev, V. F. Zolin, and Ch. M. Briskina, Kvantovaya Elektron. (Moscow) **13**, 427 (1986) [Sov. J. Quantum Electron. **16**, 281 (1986)]; C. Guedard *et al.*, J. Opt. Soc. Am. B **10**, 2358 (1993).
- [3] N. M. Lawandy *et al.*, Nature (London) **368**, 436 (1994); H. Cao *et al.*, Phys. Rev. Lett. **82**, 2278 (1999); S. V. Frolov, Z. V. Vardeny, and K. Yoshino, Phys. Rev. B **57**, 9141 (1999).
- [4] S. John and G. Pang, Phys. Rev. A **54**, 3642 (1996).
- [5] D. S. Wiersma and A. Lagendijk, Phys. Rev. E **54**, 4256 (1996).
- [6] G. A. Berger, M. Kempe, and A. Z. Genack, Phys. Rev. E **56**, 6118 (1997).
- [7] T. S. Misirpashaev and C. W. J. Beenakker, Phys. Rev. A **57**, 2041 (1998).
- [8] X. Y. Jiang and C. M. Soukoulis, Phys. Rev. Lett. **85**, 70 (2000).
- [9] C. Vanneste and P. Sebbah, Phys. Rev. Lett. **87**, 183903 (2001).
- [10] A. L. Burin *et al.*, Phys. Rev. Lett. **88**, 093904 (2002).
- [11] V. M. Apalkov, M. E. Raikh, and B. Shapiro, Phys. Rev. Lett. **89**, 016802 (2002).
- [12] A. L. Burin *et al.*, J. Opt. Soc. Am. B **21**, 121 (2004).
- [13] O. J. Painter *et al.*, Science **284**, 1819 (1999); N. Susa, IEEE J. Quantum Electron. **37**, 1420 (2001); P. R. Villeneuve, S. Fan, and J. D. Joannopoulos, Phys. Rev. B **54**, 7837 (1996); K. Sakoda, J. Appl. Phys. **84**, 1210 (1998); S. Noda, A. Chutinan, and M. Imada, Nature (London) **407**, 608 (2000).
- [14] R. C. McPhedran *et al.*, Aust. J. Phys. **52**, 791 (1999).
- [15] S. Nojima, Appl. Phys. Lett. **79**, 1959 (2001).
- [16] A. Taflove and S. C. Hagness, *Computational Electrodynamics*, 2nd ed. (Artech House, Boston, 2000).
- [17] A. L. Burin *et al.*, Phys. Rev. Lett. **87**, 215503 (2001).
- [18] J. P. Dowling *et al.*, J. Appl. Phys. **75**, 1896 (1994).
- [19] K. Sakoda, K. Ohtaka, and T. Ueta, Opt. Express **4**, 481 (1999).
- [20] V. I. Kopp *et al.*, Opt. Lett. **23**, 1707 (1998).
- [21] N. Susa, Jpn. J. Appl. Phys., Part 1 **40**, 142 (2001).
- [22] H.-Y. Ryu, S.-H. Kwon, Y.-J. Lee, Y.-H. Lee, and J.-S. Kim, Appl. Phys. Lett. **80**, 3476 (2002).
- [23] J. M. Frigerio, J. Rivory, and P. Sheng, Opt. Commun. **98**, 231 (1993).
- [24] S. Fan, P. R. Villeneuve, and J. D. Joannopoulos, J. Appl. Phys. **78**, 1415 (1995); A. A. Asatryan *et al.*, Phys. Rev. E **62**, 5711 (2000); M. M. Sigalas *et al.*, Phys. Rev. B **59**, 12767 (1999); Z. Y. Li and Z. Q. Zhang, *ibid.* **62**, 1516 (2000).
- [25] R. M. Balachandran, N. M. Lawandy, and J. A. Moon, Opt. Lett. **22**, 319 (1997).
- [26] M. Siddique *et al.*, Opt. Lett. **21**, 450 (1996).
- [27] M. N. Shkunov *et al.*, Synth. Met. **116**, 485 (2001); Adv. Funct. Mater. **12**, 21 (2002).